



The Role of the FMN-Domain of Human Cytochrome P450 Oxidoreductase in Its Promiscuous Interactions With Structurally Diverse Redox Partners

Francisco Esteves^{1*}, Diana Campelo¹, Bruno Costa Gomes¹, Philippe Urban², Sophie Bozonnet², Thomas Lautier², José Rueff¹, Gilles Truan² and Michel Kranendonk^{1*}

¹ Centre for Toxicogenomics and Human Health (ToxOmics), Genetics, Oncology and Human Toxicology, NOVA Medical School, Faculty of Medical Sciences, Universidade NOVA de Lisboa, Lisbon, Portugal, ² Centre National de la Recherche Scientifique, Institut National de la Recherche Agronomique, Institut National des Sciences Appliquées de Toulouse, Toulouse Biotechnology Institute, Université de Toulouse, Toulouse, France

OPEN ACCESS

Edited by:

Miia Turpeinen,
Oulu University Hospital, Finland

Reviewed by:

Ayyalusamy Ramamoorthy,
University of Michigan, United States
Evgeniy Yablokov,
Russian Academy of Medical
Sciences (RAMS), Russia
James Robert Reed,
Louisiana State University,
United States

*Correspondence:

Francisco Esteves
francisco.esteves@nms.unl.pt
Michel Kranendonk
michel.kranendonk@nms.unl.pt

Specialty section:

This article was submitted to
Drug Metabolism and Transport,
a section of the journal
Frontiers in Pharmacology

Received: 26 September 2019

Accepted: 28 February 2020

Published: 18 March 2020

Citation:

Esteves F, Campelo D, Gomes BC, Urban P, Bozonnet S, Lautier T, Rueff J, Truan G and Kranendonk M (2020) The Role of the FMN-Domain of Human Cytochrome P450 Oxidoreductase in Its Promiscuous Interactions With Structurally Diverse Redox Partners. *Front. Pharmacol.* 11:299. doi: 10.3389/fphar.2020.00299

NADPH cytochrome P450 oxidoreductase (CPR) is the obligatory electron supplier that sustains the activity of microsomal cytochrome P450 (CYP) enzymes. The variant nature of the isoform-specific proximal interface of microsomal CYPs indicates that CPR is capable of multiple degenerated interactions with CYPs for electron transfer, through different binding mechanisms, and which are still not well-understood. Recently, we showed that CPR dynamics allows formation of open conformations that can be sampled by its structurally diverse redox partners in a CYP-isoform dependent manner. To further investigate the role of the CPR FMN-domain in effective binding of CPR to its diverse acceptors and to clarify the underlying molecular mechanisms, five different CPR-FMN-domain random mutant libraries were created. These libraries were screened for mutants with increased activity when combined with specific CYP-isoforms. Seven CPR-FMN-domain mutants were identified, supporting a gain in activity for CYP1A2 (P117H, G144C, A229T), 2A6 (P117L/L125V, G175D, H183Y), or 3A4 (N151D). Effects were evaluated using extended enzyme kinetic analysis, cytochrome *b*₅ competition, ionic strength effect on CYP activity, and structural analysis. Mutated residues were located either in or adjacent to several acidic amino acid stretches – formerly indicated to be involved in CPR:CYP interactions – or close to two tyrosine residues suggested to be involved in FMN binding. Several of the identified positions co-localize with mutations found in naturally occurring CPR variants that were previously shown to cause CYP-isoform-dependent effects. The mutations do not seem to significantly alter the geometry of the FMN-domain but are likely to cause very subtle alterations leading to improved interaction with a specific CYP. Overall, these data suggest that CYPs interact with CPR using an isoform specific combination of several binding motifs of the FMN-domain.

Keywords: NADPH cytochrome P450 oxidoreductase (CPR), cytochrome P450 monooxygenases (CYP), FMN-domain, binding motifs, redox partner, protein–protein interaction, electron transfer

INTRODUCTION

NADPH cytochrome P450 oxidoreductase (CPR) is the crucial electron donor of all microsomal cytochrome P450s (CYPs), involved in drug and xenobiotic metabolism, but also in other key biochemical processes such as cholesterol and fatty acid homeostasis and steroid hormone biosynthesis (Guengerich, 2015). Moreover, CPR is also the unique electron donor of more structurally divergent enzymes such as heme oxygenase and squalene monooxygenase (Ellis et al., 2009; Pandey and Flück, 2013; Waskell and Kim, 2015). The interaction between CPR and microsomal CYPs promotes a two electron transfer (ET) from NADPH through the CPR cofactors FAD (reductase) and FMN (transporter) to the heme iron of CYP (reviewed in, Waskell and Kim, 2015). CPR contains a hydrophobic N-terminal transmembrane segment, responsible for its association and orientation in the endoplasmic reticulum (ER). The highly flexible hinge region which links the FMN-binding domain to the FAD/NADPH-binding domain, is involved in the transition between CPR's closed/locked (inter-flavin electron transfer) and open/unlocked (electron donation) conformations (Aigrain et al., 2009; Ellis et al., 2009; Hamdane et al., 2009; Sündermann and Oostenbrink, 2013; Frances et al., 2015; Campelo et al., 2017). The hinge region has been suggested to be largely responsible for the formation of diverse multiple open conformations, involved in the formation of productive enzyme complexes, in an apparent CYP isoform dependent manner (Campelo et al., 2018).

It has been a longstanding and intriguing issue how CPR is able to interact and sustain the activity of so many structurally diverse partners in its ET function (Kandel and Lampe, 2014; Hlavica, 2015). Charge pairing and van der Waal's interactions have been implicated in this affinity sampling, indicating that both electrostatic and hydrophobic interactions are to be considered necessary for complex formation (Waskell and Kim, 2015). The importance of affinity in the formation of an effective enzyme complex is emphasized by the *in vivo* existence of CPR:CYP stoichiometry's in favor of CYP, implying competition between individual CYP isoforms in binding to CPR in the ER (Kranendonk et al., 2008; Campelo et al., 2018). Therefore, the effective ET from CPR to structurally diverse redox partners seems to be enabled by: (1) the existence of multiple open conformations, the result of CPR's open/closed dynamics, that can be sampled by its diverse redox partners; (2) affinity probing of these open conformers, guided by CYP-isoform specific affinity for the FMN-domain of CPR, to achieve effective docking of acceptors with CPR. Additionally, several earlier studies have suggested that the CPR transmembrane segment, mostly helical, could be implied in the preliminary association of the CPR with CYPs, mediated by their respective N-terminal transmembrane segments (Black et al., 1979; Gum and Strobel, 1981; Black and Coon, 1982; Bernhardt et al., 1983; Miyamoto et al., 2015).

Abbreviations: C7H, coumarin 7-hydroxylation; CPR, NADPH cytochrome P450 oxidoreductase; CYB5, cytochrome *b*₅; CYP, cytochrome P450; DBODE, dibenzylfluorescein *O*-debenzylation; ET, electron transfer; ER, endoplasmic reticulum; EROD, ethoxy-resorufin *O*-deethylation; FAD, flavin adenine dinucleotide; FMN, flavin mononucleotide; MD, molecular dynamics; MROD, methoxy-resorufine *O*-demethylation; Mut, mutant; wt, wild type.

Moreover, the role of lipids and membrane anchoring of CPR and CYP have been recently confirmed to be of importance in the effectiveness of CPR's ET (Barnaba et al., 2017; Campelo et al., 2017; Denisov and Sligar, 2017; Barnaba and Ramamoorthy, 2018).

The FMN-domain acts as the interface for ET to all CPR's structurally diverse redox partners, including the 50 human microsomal CYP isoforms (Gutierrez et al., 2002; Hlavica and Lehnerer, 2010; Kandel and Lampe, 2014). This domain is highly conserved across species (Pandey and Flück, 2013) and it consists of a five-stranded parallel β -sheet in the core fold, flanked by α -helices with the FMN cofactor positioned at the tip of the C-terminal side of the β -sheet (reviewed in, Hlavica, 2015). The FMN-domain has several conserved patches of acidic residues on its solvent exposed surface, suggested to be involved in the electrostatic interaction with its ET partners (reviewed in, Hlavica, 2015; Waskell and Kim, 2015). Several studies questioned the role of specific residues involved in FMN binding (Shen et al., 1989; Marohnic et al., 2010) and in the interaction of CPR with its redox partners (Strobel et al., 1989; Nadler and Strobel, 1991; Shen and Kasper, 1995; Bridges et al., 1998; Hamdane et al., 2009). In these works CPR mutants, produced by site directed mutagenesis or chemically modified CPR variants, were used in structural and functional analysis of residues of the CPR-FMN domain. The importance of specific residues in the vicinity of the FMN binding domain was demonstrated as well as the role of acidic amino acids in CPR's binding to its electron acceptors, however identification of these residues was dependent on which CPR: acceptor couple was studied (Hlavica et al., 2003). Three distinct clusters of acidic residues were indicated to be involved in CPR's interaction with multiple redox-partners (Shen and Strobel, 1994; Zhao et al., 1999). Electrostatic potential surface analysis revealed basic residues on the proximal side of CYPs (Waskell and Kim, 2015). These are thought to steer the geometrically convex FMN-domain of CPR through its negatively charged patches to CYP's concave docking site near the heme moiety (Williams et al., 2000; Hlavica and Lehnerer, 2010). However, microsomal CYPs do not demonstrate signature sequences of these basic residues at their proximal side, a feature displayed by mitochondrial CYPs in the interaction with their redox partner iron-sulfur protein adrenodoxin (Pikuleva et al., 1999). This suggests that CPR interacts with microsomal CYPs in an isoform-dependent manner, which we demonstrated recently (Campelo et al., 2018). Thus CPR has a degenerated binding site for interaction with its diverse electron acceptors, but besides the suggested involvement of the conserved negatively charged patches, it is so far unclear what features of the FMN-domain enable CPR to interact with so many structural diverse redox partners in its ET function.

The present study describes the search for structural features of CPR's FMN-domain, responsible for its degenerated interaction with CYPs, for effective sampling of open conformations. This was accomplished through the isolation and study of FMN-domain mutants selected for increased CYP activity when combined with specific isoforms. These mutations, expected to lead to improved interaction of CPR with these CYPs, should be informative on the localization and nature of features

required for this “one-serve-all”-type of interaction. Random mutation libraries of the FMN-domain in full length human CPR were created, with increasing mutation frequencies. Each of these libraries was combined with three representative human drug metabolizing CYP isoforms (Guengerich, 2015), phylogenetically apart, namely CYP1A2, 2A6, or 3A4¹. Mutant CPR-pools were co-expressed with each of these three CYPs in a dedicated bacterial cell model and screened for increased CYP-activity, using our recently developed whole-cell high-throughput activity assay (Esteves et al., 2018). Using membrane fractions of selected clones, detailed enzyme kinetic analysis, study of ionic strength effect and cytochrome *b*₅ (CYB5) competition were performed, to confirm improved interaction. Structural analyses were carried out to rationalize the role of the mutated FMN-domain residues in the CPR:CYP degenerate interaction. Collectively, our data seems to indicate that each CYP interacts with CPR in a isoform specific manner, involving specific combinations of binding motifs of the FMN-domain which were formerly identified to be involved in the CPR:CYP interactions.

MATERIALS AND METHODS

Reagents

L-Arginine, thiamine, chloramphenicol, ampicillin, kanamycin sulfate, isopropyl β-D-thiogalactoside (IPTG) (dioxane-free), δ-aminolevulinic acid, glucose 6-phosphate, glucose 6-phosphate dehydrogenase, nicotinamide adenine dinucleotide phosphate (NADP⁺ and NADPH) were obtained from Sigma-Aldrich (St. Louis, MO, United States). LB Broth, bacto tryptone and bacto peptone were purchased from BD Biosciences (San Jose, CA, United States). Bacto yeast extract was obtained from Formedium (Norwich, United Kingdom). Ethoxyresorufin, methoxyresorufine and coumarin were obtained from BD Biosciences (San Jose, CA, United States) and dibenzylfluorescein from Santa Cruz Biotechnology (Santa Cruz, CA, United States). Resorufin, 7-hydroxy coumarin, fluorescein and dichlorophenolindophenol (DCPIP) were obtained from Sigma-Aldrich (St. Louis, MO, United States). A polyclonal antibody from rabbit serum raised against recombinant human CPR obtained from Genetex (Irvine, CA, United States) was used for immune-detection of the membrane-bound CPR. All other chemicals and solvents were of the highest grade commercially available.

Construction of the CPR-FMN-Domain Mutant-Libraries

CPR mutant pools were constructed with controlled random mutation rates targeting the FMN-domain of CPR. Random mutants were produced using as a template the sub-cloning vector pUC_POR, containing the initial segment (1–1269 bp) of human *POR* cDNA (based on NCBI sequence NM_000941.3, encoding the CPR consensus protein sequence NP_000932.3). Error-prone PCR (epPCR) (McCullum et al., 2010) was used

for random mutagenesis of the FMN-domain sequence using GeneMorph II Random Mutagenesis Kit (Agilent, Santa Clara, CA, United States), with primers AdRandom POR Fw and AdRandom POR Rv (see **Supplementary Table S1**), which yielded a 822 bp fragment encompassing the FMN-domain. Error-prone PCR reactions were as follows: 30 cycles at 95°C for 30 s, 55°C for 30 s, and 72°C for 1 min, and a final extension at 72°C for 10 min (GeneAmp PCR System 9700; Applied Biosystems, Foster City, CA, United States), using 0.5 μM of each primer, pUC_POR as template (ranging from 0.1 to 1.9 μg), 2.5 U Mutazyme II DNA polymerase (Agilent), 1x reaction buffer (Mutazyme II reaction buffer; Agilent), 0.2 mM of each deoxynucleoside triphosphates (dNTPs) (Thermo Fisher Scientific, Waltham, MA, United States), in a 50 μl final reaction volume. CPR-FMN mutant pools were characterized for their mutation frequencies (mutant/FMN-domain fragment) by direct sequencing of the epPCR amplicons of the *POR* fragments, with primers AdRandom POR Fw and AdRandom POR Rv. Sequences were aligned and analyzed (position-numbering was based on NCBI consensus sequences NM_000941.3) using BLAST (version 2.3) (NCBI) and MultAlin (French National Institute for Agricultural Research, Centre Toulouse Midi-Pyrénées). Five different libraries were generated with increasing mutation frequencies (see **Supplementary Table S2**).

The five pools of the mutated FMN-domain segments present in pUC_POR were cloned into the human full-length wild type CPR expression vector pLCM_POR_{wt} (Kranendonk et al., 2008), through *EcoRI* + *AatII* digestion followed by ligation with T4 DNA Ligase (Rapid DNA Ligation Kit, Thermo Fisher Scientific). Alternatively, mutated fragments were used as mega-primers and cloned back into plasmid pLCM_POR using mega-primer PCR of the whole plasmid (mwPCR) (Miyazaki, 2011), followed by purification (GeneJET PCR Purification Kit, Thermo Fisher Scientific) and *DpnI* treatment (Thermo Fisher Scientific). The five FMN-domain mutant-libraries, harbored in the pLCM_POR plasmid were used to transform *E. coli* PD301 (Duarte et al., 2005, 2007), already containing the expression vector (pCWori) (Fisher et al., 1992) for human CYP1A2, 2A6, or 3A4 (expressed in N-terminal modified forms), through standard electroporation procedures, creating a total of 15 different libraries (Observation: from here on clones containing CPR with mutations in the FMN-domain, combined with a human CYP present in BTC bacteria are simply designated as CPR_{mut}/CYP versus when containing wild type CPR: CPR_{wt}/CYP).

CPR_{mut}/CYP clones were picked from overnight grown LB agar-plates supplemented with chloramphenicol 10 μg/L, ampicillin 50 μg/L and kanamycin 15 μg/L, and transferred to single wells of flat-bottom 96-well microplates (CoStar, Washington, DC, United States), previously filled with 200 μl LB broth supplemented with antibiotics (see above). This procedure was partially executed with the use of a Biomek 2000 Laboratory Automation Workstation (Beckman Coulter; Brea, CA, United States) and the Kbiosystems K2 automated colony picker system (Kbiosystems; Basildon, Essex, United Kingdom). Culture microplates were incubated at 37°C, for 16 h with agitation (250 rpm), and subsequently supplemented with 10% glycerol and stored at –80°C.

¹<https://drnelson.uthsc.edu/fuguhum.tree.pdf>

High-Throughput Screening of CPR-FMN-Domain Mutant-Libraries

Stored (-80°C) cultures were transferred by replicate plating to new flat-bottom 96-well microplates, previously filled with 200 μl LB broth supplemented with antibiotics (see above) and incubated at 37°C , for 16 h, at 250 rpm. Subsequently, 50 μl of the grown cultures was used to inoculate a 96-deep well plate (VWR, Radnor, PA, United States), previously filled with 1400 μl TB medium, pH 7.5 (except for the CYP3A4 containing strains cultured at pH 6.8), supplemented with designated antibiotics (see above), 2 g/L peptone, 1 mg/L thiamine, 0.04% (v/v) trace elements solution, IPTG 0.2 mM, δ -aminolevulinic acid 0.05 mM (CYP1A2 expressing clones) or 0.1 mM (CYP2A6 and CYP3A4 clones). Cultures were grown at 27°C , at 310 rpm agitation for 22 h, using gas-permeable membranes (Greiner bio-one, Kremsmünster, Austria).

CYP content of individual well-cultures was determined using the method described by Otey (2003) and Johnston et al. (2008), with minor modifications. Briefly, bacterial cells were harvested and washed twice with PBS buffer (pH 7.4) and re-suspended in 200 μl of the same buffer, containing 1 mg/ml sodium dithionite, hence obtaining a sevenfold concentrated cell-suspension. Whole-cell CYP content was determined in a flat-bottom 96-well microplate using a SpectraMax i3x microplate reader (Molecular Devices, Silicon Valley, CA, United States), measuring absorbance at 436, 450, 470, and 490 nm. Cells suspensions were then subjected to 100% CO-atmosphere for 15 min in a gas-tight bag before performing the second reading at the same wavelengths to record the reduced, CO-bound CYP absorbance. CYP contents were calculated using the equation previously mentioned (Johnston et al., 2008).

CYP1A2, 2A6, or 3A4 activities in whole-cells were assayed using the high-throughput CYP-activity assay described in our recent report (Esteves et al., 2018). Observed rate constants (k_{obs}) [pmol of fluorescent product formed/(pmol of CYP per minute)] were measured. Cultures of CPR_{wt}/CYP and CPR_{null}/CYP were used as controls in all experiments. Control strains were obtained for each CYP (1A2, 2A6, or 3A4): one expressing CPR_{wt}, through expression plasmid pLCM_POR_{wt}, or with the mock plasmid pLCM (lacking POR cDNA), each combined with the respective human CYP expression plasmid (pCW_CYP) (Kranendonk et al., 1998; Palma et al., 2013). Clones demonstrating reaction velocities above 110%, i.e., an increase above two times background variation (5%), were selected.

Identification of CPR-FMN-Domain Mutations

Plasmid DNA was isolated from overnight cultures of selected CPR_{mut}/CYP clones using GeneJET Plasmid Miniprep Kit (Thermo Fisher Scientific). The cDNA encoding full length human CPR of isolated clones was extensively sequenced, using four sequencing primers (see **Supplementary Table S1**) for identification of FMN-domain mutations and to rule out any potential undesired additional mutations in other segments of the POR cDNA. Sequences were aligned and analyzed as described above.

Enzyme Activity Evaluation Using Membrane Fractions

Membrane fractions of selected CPR_{mut}/CYP clones were prepared and characterized for CYP- (CO-difference spectrophotometry), CPR- (immune-detection by western blotting) and protein-contents (Bradford assay), using previously described methods (Duarte et al., 2007; Kranendonk et al., 2008; Moutinho et al., 2012; Palma et al., 2013; Campelo et al., 2018; Esteves et al., 2018). The intrinsic electron donation capacity of the CPR-FMN-domain mutants was assessed by DCPIP reduction. These assays were performed in a buffer containing 50 mM Tris, 150 mM KCl, 10 mM NaN₃, 0.04% Triton X-100, pH 7.5 at 37°C in the presence of 200 μM NADPH and 70 μM DCPIP. Initial rates were monitored at 600 nm using $\Delta\epsilon_M = 21,000 \text{ M}^{-1} \text{ cm}^{-1}$ (Campelo et al., 2017).

The catalytic activities of CYP1A2, 2A6, or 3A4, sustained by CPR-FMN-domain mutants were evaluated as reported previously (Palma et al., 2010; Campelo et al., 2018). Initial velocities were measured in triplicate and plots of velocity traces *versus* substrates concentrations could be fitted according to the Michaelis-Menten equation ($r^2 \geq 0.95$) to determine steady-state kinetic parameters, using GraphPad Prism 5.01 Software (La Jolla, CA, United States) (Kranendonk et al., 2008; Moutinho et al., 2012; Campelo et al., 2018; Esteves et al., 2018).

CYB5 Competition and Ionic Strength Effect

Full length human CYB5 was expressed in *E. coli* BL21-DE3 and purified as reported by Campelo et al., 2018. The effect of CYB5 and salt concentrations on CYP1A2, 2A6, or 3A4 activities, sustained by CPR-FMN-domain mutants, was assessed through microtiter plate approaches, as described previously (Campelo et al., 2018). All reaction velocities (k_{obs}) were measured at least in triplicate [pmol of fluorescent product formed/(pmol of CYP per minute)].

Multiple Alignment of CPR Mutants

Sequences of CPR proteins were downloaded from Universal Protein Resource (UniProt)², aligned and analyzed (position-numbering was based on NCBI consensus sequences NM_000941.3) using the AliView software version 1.25 (Department of Systematic Biology, Uppsala University, Sweden). The alignment was performed with the MUSCLE algorithm from the AliView embedded routine.

Structural Analysis of CPR Mutants

The structural analysis of three mutants (P117H, G144C, and A229T) was performed using the crystal structure PDB 5FA6 of the FMN-domain of human CPR_{wt} as the starting material. Mutations were constructed with the YASARA software³ and two independent molecular dynamics simulations were run at 298 K for 24 ns, using the AMBER14 force field, with 0.9% NaCl and pH 7.4. Snapshots of the simulation were taken every 100 ps. The

²www.uniprot.org

³www.yasara.org

YASARA software was used to calculate the coordinates of the average molecule for the WT and mutants and the root mean square fluctuation (RMSF) deviations calculated for each atom introduced as B factors.

Statistical Analysis

Variance in data was analyzed through one-way ANOVA with Bonferroni's multiple comparison test. The unpaired Student's *t*-test was performed for calculation of the two-tailed *P*-value. The analysis was performed with 95% confidence interval using the GraphPad Prism 5.01 Software. The significance level considered in all the statistical tests was 0.05.

RESULTS

Creation of CPR-FMN-Domain Mutant-Libraries

Libraries of the FMN-domain section of the cDNA of the *POR* gene carrying random mutations were generated with increasing frequencies, namely 0.9, 1.0, 1.2, 1.3, and 1.4 mutations per FMN-domain segment (**Supplementary Figure S1**). The mutated cDNA stretches of each set, were cloned back in the human CPR expression vector pLCM_POR (Kranendonk et al., 2008), creating five libraries for full-length CPR expression with different extents of mutagenesis restricted to the FMN-domain. Each of these random CPR-FMN-domain mutant-libraries was combined separately with three different CYP expression plasmids, for human isoforms CYP1A2, 2A6, or 3A4. CPR-FMN-domain mutants and CYPs were expressed using the dedicated *E. coli* strain, BTC, containing the specialized bi-plasmid system adequate for co-expression of CPR with representative human CYPs (Duarte et al., 2005, 2007). As such, a total of 15 BTC CPR_{mut}/CYP libraries with CPR-FMN-domain mutant frequencies ranging from 0.9 to 1.4, were generated (**Supplementary Table S2**).

Screening of CPR-FMN-Domain Mutant-Libraries

From the 15 libraries, a total of 2376 CPR_{mut}/CYP clones were screened, using our recently developed whole-cell high-throughput activity assay (Esteves et al., 2018). With this approach, CYP-expression levels may vary from clone to clone (due to difference in expression between different wells of the microtiter plate), interfering with the detection of CPR variants, supporting increased CYP activity. Therefore rates of product formation were normalized with measured CYP expression levels from each clone. CPR_{mut}/CYP clones were selected when presenting a 10% or more increase in turnover rates, when compared to the parental clones containing wild type CPR. This cutoff was selected based on the experimental setup in which turnover rates of the CPR_{wt}/CYP strains demonstrated standard deviations from average values, well below 10% determined with preliminary assays (data not shown). From the 2376 CPR_{mut}/CYP clones screened, seven were selected due to enhanced CYP activities (k_{obs} increase ranging from 1.2 to

7.25 × fold) (**Supplementary Figure S2**). The cDNA of CPR of each of these seven clones was subsequently sequenced to identify their FMN-domain mutations. A total of seven mutations (six single and one double mutant) were identified (**Table 1**).

Detailed Enzyme Activity Characterization of BTC CPR_{mut}/CYP Clones

Membrane fractions were isolated from the selected seven CPR_{mut}/CYP clones for confirmation of increased CYP activity and for further detailed analysis. Characterization of contents of heterologous expressed proteins from the selected seven CPR_{mut}/CYP clones is shown in **Table 1**. The CPR:CYP stoichiometries measured in membrane fractions were similar to those described previously for the BTC system in our former studies, when expressing CYP1A2, 2A6 or 3A4, and comparable with the ranges found physiologically (Duarte et al., 2005, 2007; Moutinho et al., 2012; Palma et al., 2013; McCammon et al., 2016; Campelo et al., 2018; Esteves et al., 2018). Co-expression of the mutant CPRs with CYP1A2, 2A6, or 3A4 was achieved with a stoichiometry approximating the one obtained with CPR_{wt} for each CYP, demonstrating no significant differences ($P > 0.05$). The only exception was found for the A229T CPR variant, for which the CPR:CYP1A2 ratio was approximately three times smaller when compared to CPR_{wt}. Thus, the data of this mutant was interpreted subsequently with caution.

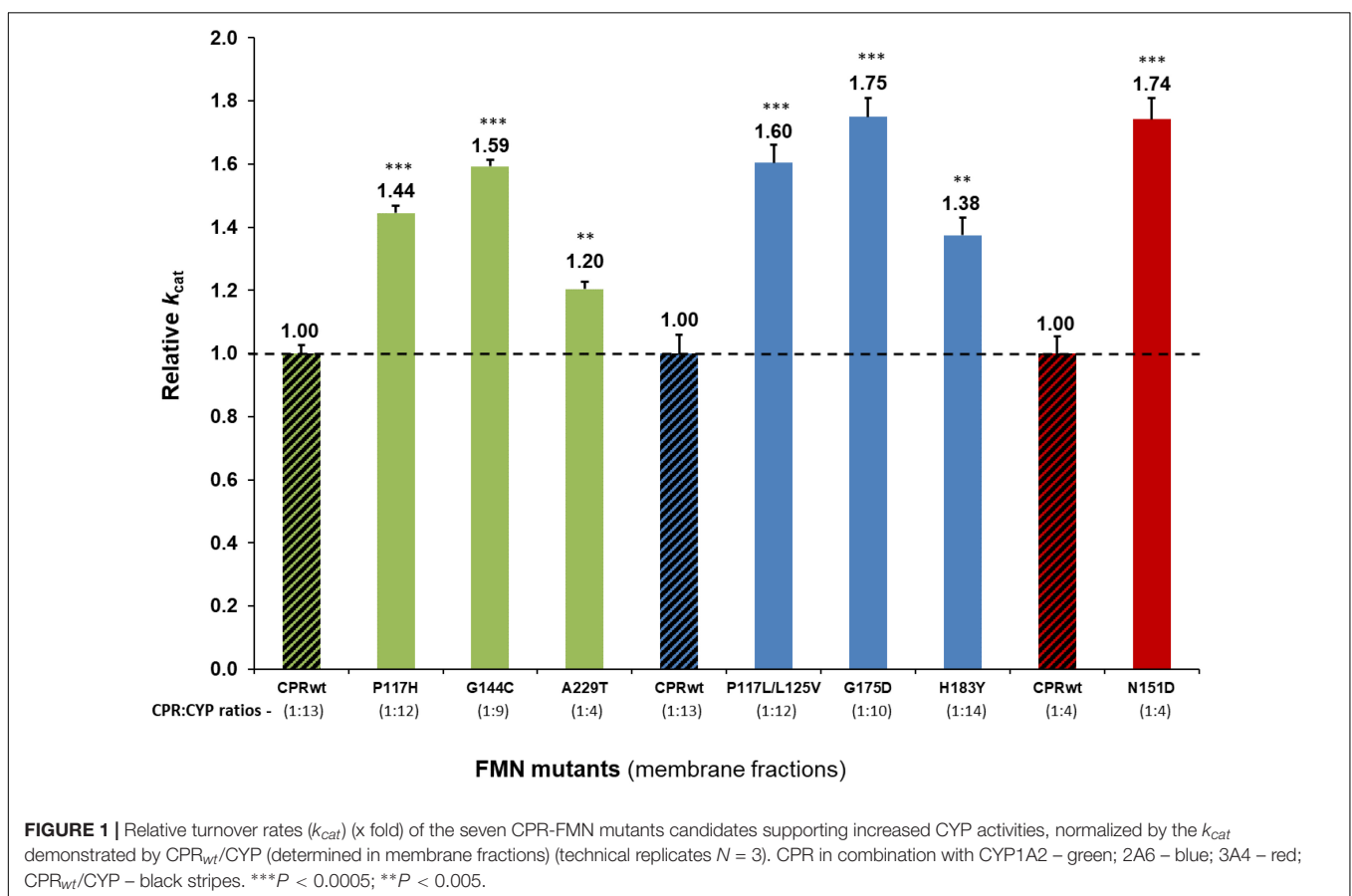
Detailed analysis using membrane preparations confirmed enhanced turnover rates (k_{cat}) of the seven selected CPR_{mut}/CYP candidates, when compared to those measured with CPR_{wt}/CYP (**Figure 1** and **Supplementary Table S3**). To further verify if augmented reaction velocities are due to improved CPR:CYP interaction and not to altered FMN content and/or change in redox-potential of FMN in CPR_{mut}, the reduction rates of DCPIP were measured. This assay measures the electron flow from NADPH to FAD and finally to FMN, which directly reduces DCPIP, a small chemical electron acceptor. This reaction is independent of protein:protein interaction involving the FMN-domain interface. As shown in **Table 1**, the DCPIP reduction rates of CPR_{mut} showed no significant differences when compared to CPR_{wt}, indicating no changes in the cofactors (FAD and FMN) content and redox potential for all CPR mutants. In summary, the observed differences in CYP activities for the different CPR_{mut} originate only from their improved interactions with their CYP partner, with the possible exception of the A229T mutant (*vide supra*).

The potential effect of the substrate bound on the interaction of the CPR mutants with CYP, was subsequently tested using an additional compound with CYP1A2 and its selected CPR mutants. Comparison of relative reaction velocities of CPR_{mut}:CYP1A2 using the substrate methoxy-resorufine with those formerly obtained with ethoxy-resorufine, are summarized in **Figure 2** (see additional data in **Supplementary Table S3**). CPR mutants P117H and G144C stimulated significantly the CYP1A2 mediated MROD reaction albeit less pronounced as those found for EROD. The A229T CPR mutant demonstrated no significant stimulation of the MROD reaction when compared

TABLE 1 | CYP and CPR contents of BTC membrane fractions and CPR electron donation capacity.

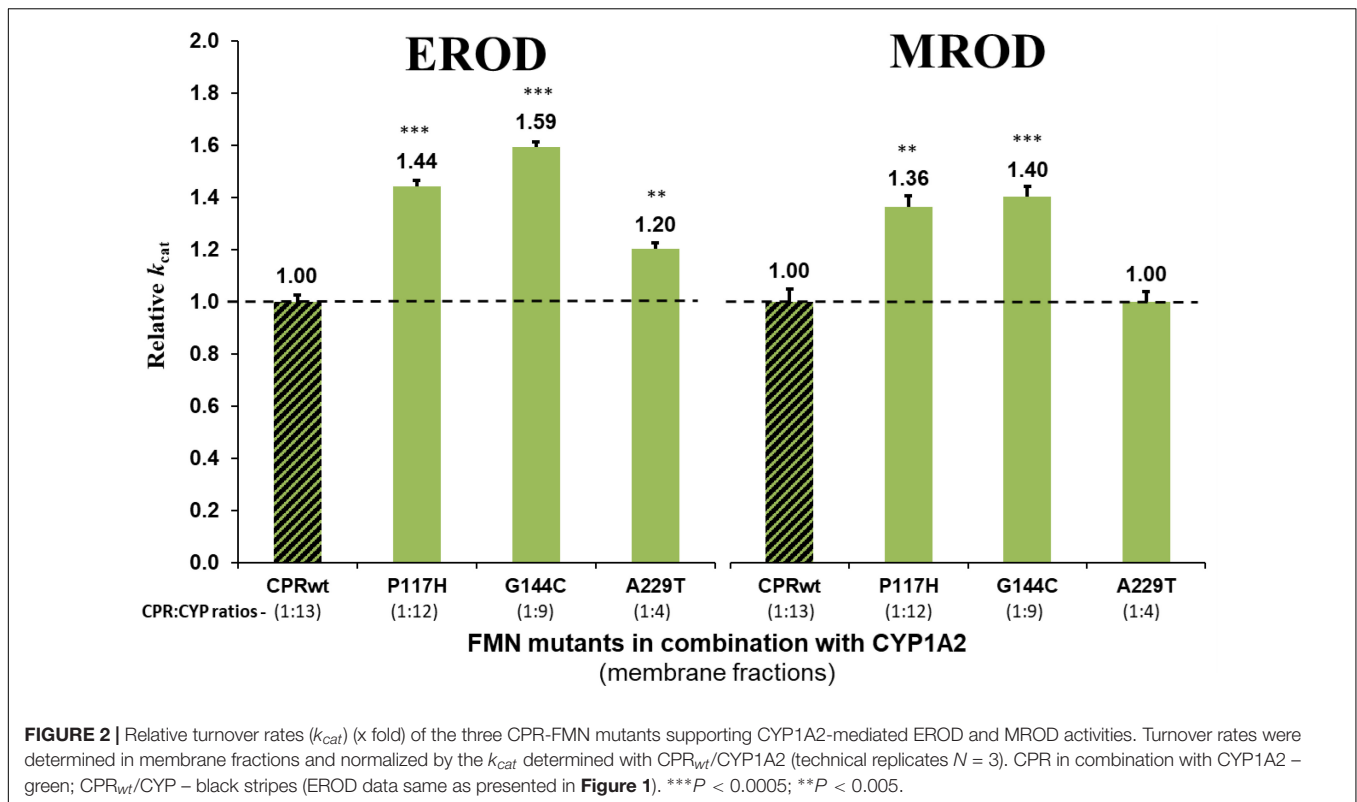
Membrane fractions		Protein contents			DCPIP reduction
CYP isoform	CPR form	CYP (pmol/mg protein)	CPR (pmol/mg protein)	CPR:CYP ratios ^a	Initial rates (min ⁻¹) ^b
CYP1A2	wt	54 ± 1	4.1 ± 1.5	1: 13	2282 ± 239
	P117H	148 ± 1	12.2 ± 0.5	1: 12	2507 ± 208
	G144C	124 ± 2	14.1 ± 0.2	1: 9	2233 ± 185
	A229T	71 ± 4	17.3 ± 0.2	1: 4	2262 ± 228
	CPR _{null}	91 ± 6	–	–	–
CYP2A6	wt	139 ± 1	10.5 ± 1.3	1: 13	2625 ± 285
	P117L/L125V	124 ± 1	10.2 ± 0.3	1: 12	2570 ± 275
	G175D	112 ± 6	11.3 ± 0.5	1: 10	2508 ± 290
	H183Y	133 ± 1	9.4 ± 0.1	1: 14	2544 ± 260
	CPR _{null}	178 ± 4	–	–	–
CYP3A4	wt	83 ± 3	19.8 ± 0.2	1: 4	2227 ± 201
	N151D	45 ± 1	12.7 ± 0.6	1: 4	2293 ± 159
	CPR _{null}	85 ± 3	–	–	–

(–) not determined. CYP and CPR contents are mean ± SD (technical replicates N = 3). The CPR_{wt}/CYP membrane fractions were from the same batch used in our former study (Campelo et al., 2018). ^aCPR:CYP ratios of the CPR_{mut} were not significantly different from the ones of the corresponding CPR_{wt} (P > 0.05), with each tested CYP. ^bNo significant differences were observed between measurements of DCPIP reduction in the membrane fractions studied.



to CPR wild type, although this was observed with EROD. This might be attributed either to the CPR_{A229T}:CYP1A2 ratio of the membrane fraction of this specific mutant, which can

be a confounding factor in the assessment of the CPR:CYP interaction or, alternatively, to a different modulation in the CPR:CYP binding by a different substrate. Thus, the EROD and



MROD results seem to confirm the improved CPR:CYP1A2 stimulation conferred by CPR_{P117H} and CPR_{G144C}. Nevertheless, the slight variations in relative k_{cat} observed for each of the CPR_{mut}:CYP1A2 couples, when tested with a different substrate, might be indicative that stimulation of CYP-mediated reactions by these CPR_{mut} may also be affected by the substrate bound.

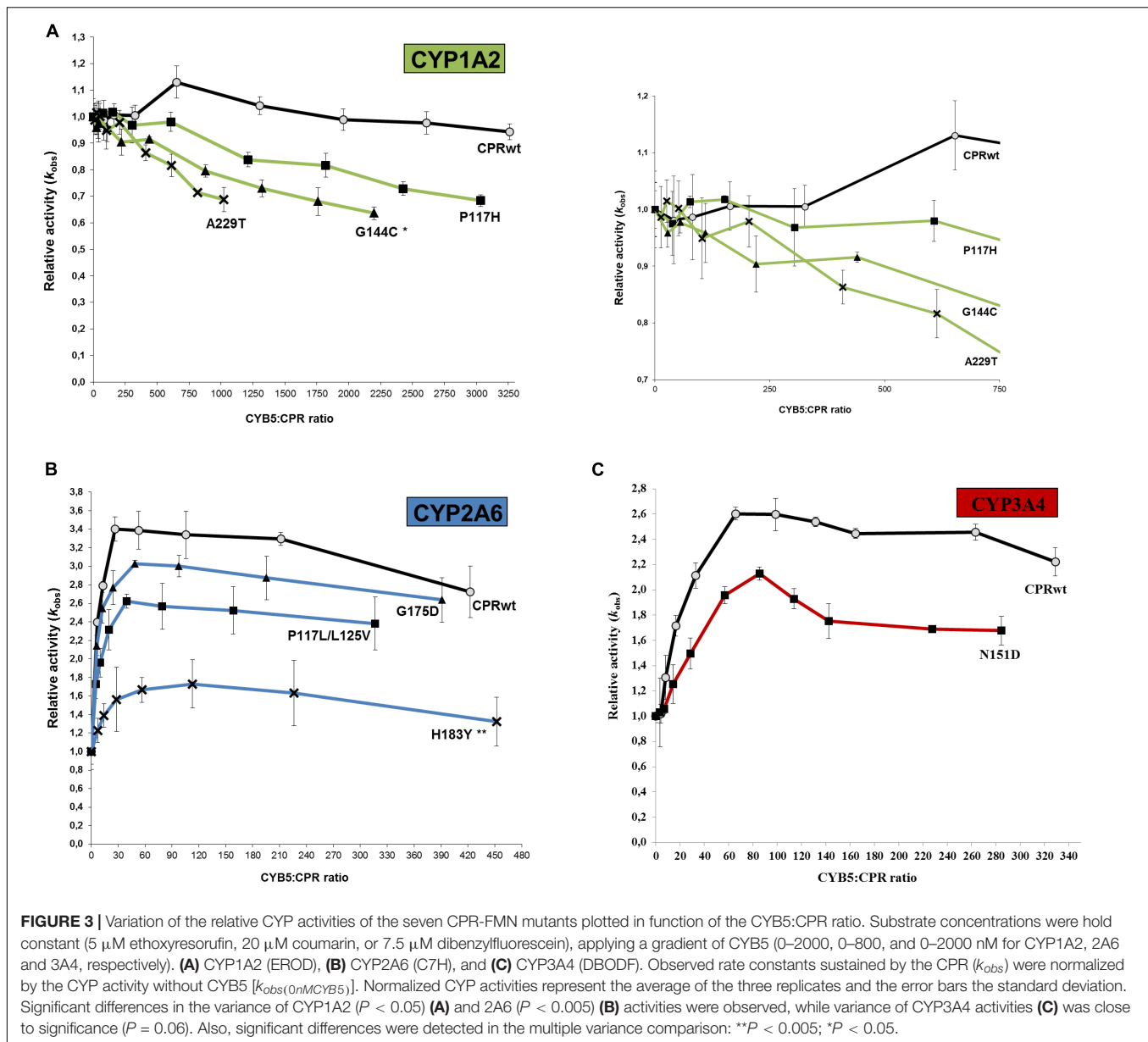
CYB5 Competition With CPR_{mut}/CYP

CPR and CYB5 bind to CYP through largely overlapping binding sites located on the proximal side of the CYP protein, predicting that these redox partners will compete for CYP with a mutually exclusive binding (Bridges et al., 1998; Zhang et al., 2007; Waskell and Kim, 2015; Gentry et al., 2018, 2019). Improvement in binding of the different FMN-domain mutants with CYP may therefore be studied by CYB5 competition experiments, similarly to what was described in our previous report on the hinge region of CPR (Campelo et al., 2018). The relative activity ratios (k_{obs} mutant/ k_{obs} wild type) were determined for the seven CPR-FMN-domain mutants with various CYB5/CPR ratios for CYP1A2, 2A6, or 3A4-mediated reactions (**Figure 3**). As demonstrated in our former study (Campelo et al., 2018), CYB5 has two putative effects on CYP-mediated reactions. The first one is present at low CYB5:CPR ratios and consists of a stimulatory effect caused by the second electron donation and/or allosteric effect, in a CYP and/or substrate dependent manner (Palma et al., 2013; Bart and Scott, 2017). The second one is the reverse effect: CYB5 can inhibit the CYP dependent reactions at high CYB5:CPR stoichiometries. The latter is caused by direct competition between CYB5 and CPR for the single binding site

on CYP, thus blocking the first electron transfer from CPR to CYPs (Waskell and Kim, 2015) or alternatively, by direct ET from CPR to CYB5, leading to reduced transfer to CYPs and thus reduced activities. However, inhibition patterns of CYB5 on the different CYPs are isoform specific and each curve obtained with CPR_{mut} follow the shape of the inhibition curves acquired with CPR_{wt}. Therefore, the inhibition pattern mediated by CYB5 cannot be attributed to the ET from CPR to CYB5. Hence, we rationalized that if a FMN-domain mutation is responsible for increased effectiveness in the docking of CPR with CYPs, it should also hamper the CYP specific CYB5 effect.

The profiles obtained from the CYB5 competition experiments showed that, in the presence of CYB5, reaction velocities of CPR_{mut}/CYP were consistently lower than those from CPR_{wt}/CYP (**Figure 3** and **Table 2**). The CYP isoform differentials CYB5-effect also coincides with the knowledge that CYP3A4 and in particular CYP2A6, are much more prone for CYB5 stimulation than CYP1A2, which is less sensitive to CYB5 for activity (Duarte et al., 2005, 2007).

The different CPR_{mut}/CYP couples demonstrated lower relative CYP reaction velocities (i.e., versus the velocity without CYB5), at low and high CYB5/CPR ratios. This was particularly true for CYP2A6 and CYP3A4 (**Figures 3B,C**) while for CYP1A2 – as CYB5 does not have a strong stimulatory effect on this isoform – only the inhibition pattern was visible (**Figure 3A** and inset of **Figure 3A**). Overall, and notwithstanding variations in the optimal stoichiometry between CYB5/CPR for activation of the CYPs activities, the stimulation (at low CYB5:CPR ratios) and inhibition (at higher CYB5:CPR ratios), are less pronounced



with all CPR_{mut} compared to CPR_{wt} . We thus can conclude that the binding of CYB5 to the different CYPs is probably greatly perturbed by the mutations present on the FMN domain of the various CPR_{mut} . Collectively, the CYB5 competition data seems to be highly indicative of improved interactions of the FMN-domain mutants with the CYP isoform (in particular CYP2A6 and CYP3A4) for which they presented increased activities (Figure 1), with the potential exclusion of the A229T mutant.

Ionic Strength Effect on $\text{CPR}_{mut}/\text{CYP}$

Previously, we studied the role of ionic strength in ET from CPR to different acceptors (Campelo et al., 2017), demonstrating that the ionic strength dependency of electron flow from CPR to the acceptors is mainly determined by the salt-dependent conformational equilibrium of CPR and, to a lesser extent,

by electrostatic interactions of the FMN-domain with the substrates/acceptors. More recently, we analyzed how ionic strength specifically modified the activity of CYP1A2, 2A6, and 3A4 (Campelo et al., 2018). CYP1A2 showed high, 3A4 intermediate and 2A6 relatively low sensitivity in their activities to varying ionic strength, indicative that CYP samples CPR's open conformations in an isoform-specific manner. Additionally, our former data corroborated the study by Yun et al. (1998), that ascribed the ionic strength effect observed mostly to CPR:CYP "interaction," while having relatively minor effects on CYP protein conformation (Yun et al., 1996).

In order to verify if the FMN-domain mutants have altered isoform specific sensitivities toward ionic strength (salt-dependent conformational equilibrium and/or electrostatic interactions with the substrates/acceptors), activities of CYPs

TABLE 2 | Effect of CYB5 and ionic strength on CPR_{mut}/CYP combinations.

CYP isoform	CPR form	CYB5 competition		Ionic strength	
		CYB5 effect (%) ^a	CYB5:CPR ratio ^b	NaCl effect (%) ^a	[NaCl] (mM) ^c
CYP1A2	CPR _{wt}	100 ± 5	652	100 ± 6	90
	CPR _{P117H}	90 ± 1	152	98 ± 6	90
	CPR _{G144C}	88 ± 3	0	93 ± 6	70
	CPR _{A229T}	90 ± 3	26	99 ± 4	70
CYP2A6	CPR _{wt}	100 ± 4	26	100 ± 10	130
	CPR _{P117L/L125V}	89 ± 1	49	95 ± 3	70
	CPR _{G175D}	77 ± 2	40	101 ± 3	70
	CPR _{H183Y}	51 ± 8	113	102 ± 2	70
CYP3A4	CPR _{wt}	100 ± 1	66	100 ± 2	170
	CPR _{N151D}	82 ± 1	85	92 ± 2	170

^aMaximum CYB5 or salt effect on CYP-activity. Normalized maximum enzyme activities (%) were determined by dividing the maximal turnover velocities of the CPR_{mut}/CYP ($k_{obs(max)} CPR_{mut}$) by the ones obtained of the corresponding CPR_{wt}/CYP ($k_{obs(max)} CPR_{wt}$). Values are expressed as the mean of three independent experiments ± SD.

^bCYB5:CPR ratio at which maximum k_{obs} was reached. ^cSalt concentration at which maximum k_{obs} was reached.

with their specific CPR mutants were tested with various NaCl concentrations (Figure 4). The CPR mutants demonstrated very similar bell-shaped salt/activity profiles for CYP1A2 (Figure 4A) and 3A4 (Figure 4C) when compared to those obtained with wild type CPR, with a strikingly similar salt concentration at which the maximal CYP-activity is obtained (Table 2). These results may indicate that the ionic strength dependent conformational equilibria of these different CPR_{mut} (P117H, G144C, A229T, and N151D) are probably not altered by the mutations and thus that the effects of the mutations are probably more related to modified interactions between CYPs and CPR_{mut}. As such, subtle changes in ionic interactions between the FMN-domain mutants and these CYPs may well be obscured by the major ionic strength effect on CPR's open/closed dynamics.

On the contrary, this was not the case for the CPR mutants obtained with CYP2A6 (Figure 4B). With NaCl concentration ranging up to 300 mM, the three CPR_{mut}/CYP2A6 activity profiles were analogous to CPR_{wt}/CYP2A6 and thus the optimal concentration of NaCl (between 50 and 150 mM) to obtain maximal velocity of CYP2A6 is undistinguishable between CPR_{wt} and CPR_{mut}. However, at ionic strength above 300 mM, all CPR_{mut} displayed increased sensitivities to ionic strength which translated into lower CYP2A6 activities. The nature of the CPR mutations, for which there is no evident pattern of electrostatic change (P to L, L to V, G to D, or H to Y), together with the fact that the increased sensitivities to ionic strength are specific to CPR_{mut} that have augmented activities with CYP2A6, may again indicate specific effects of the mutations on the recognition with CYP2A6 although effects on the open/closed dynamics of CPR cannot be totally excluded based on our former observations.

DISCUSSION

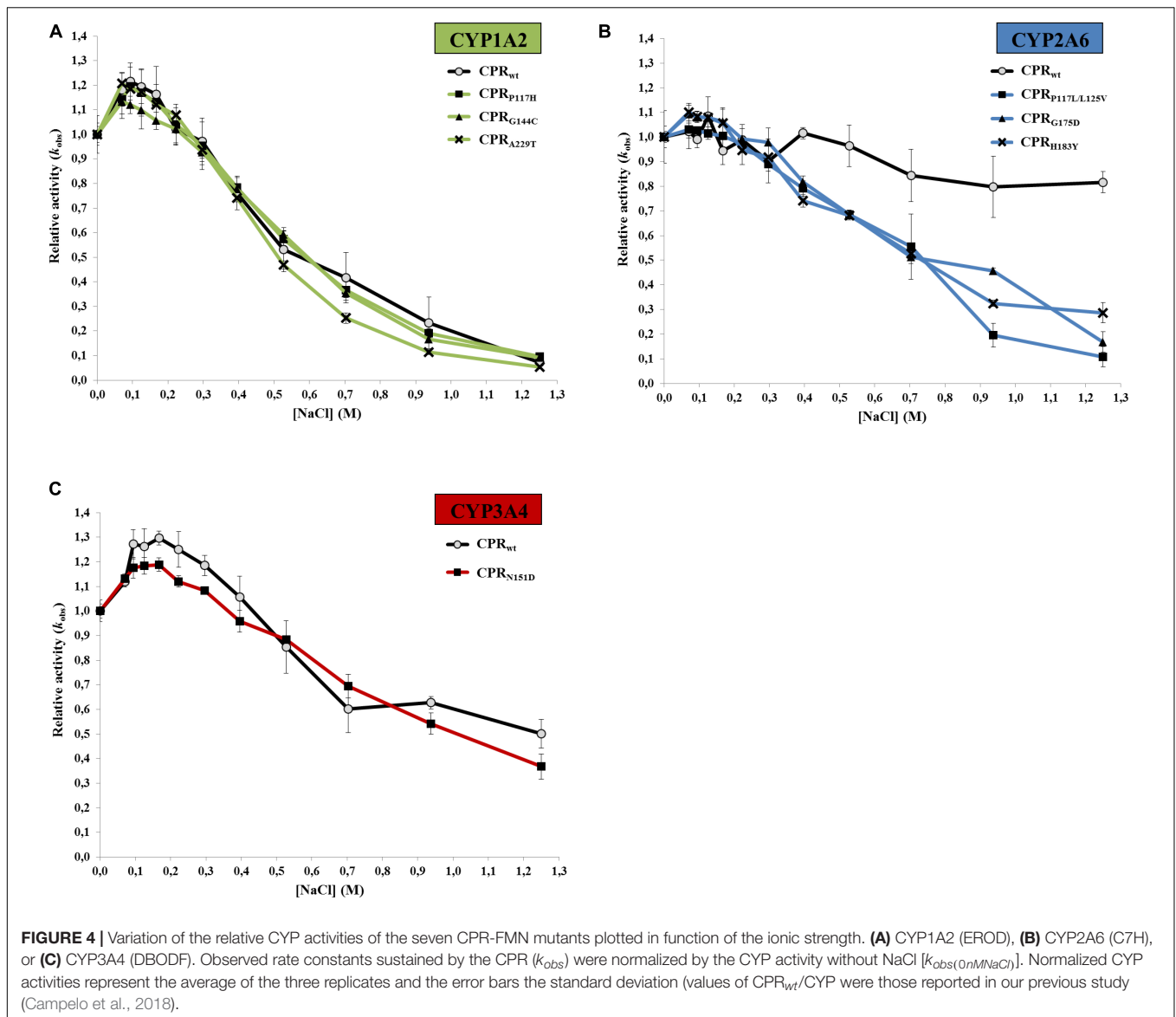
Little is known about the mechanism by which CPR selects one of its many ET partners (Waskell and Kim, 2015). It seems clear that, together with the open/close dynamics, the FMN-domain plays a central role in the docking of CPR with

CYP in the ER membrane. This raises the question how CPR, primarily through its FMN-domain, enables the affinity sampling by such a wide range of structurally diverse CYP-isoforms. This was the issue addressed by this study, using CPR variants of the FMN-domain, obtained by means of random mutagenesis. Although the size of the mutant libraries was nowhere near that of the sequence space, the success in identifying FMN-domain mutated proteins supporting a gain in CYP-activity, is indicative of a target sequence carrying densely packed functional features (Skandalis et al., 1997). This is highlighted by the high degree of conservation of this domain among species, particularly mammals (Figure 5 and Supplementary Table S4).

FMN-Domain Mutations and Their CYP-Dependent Effect

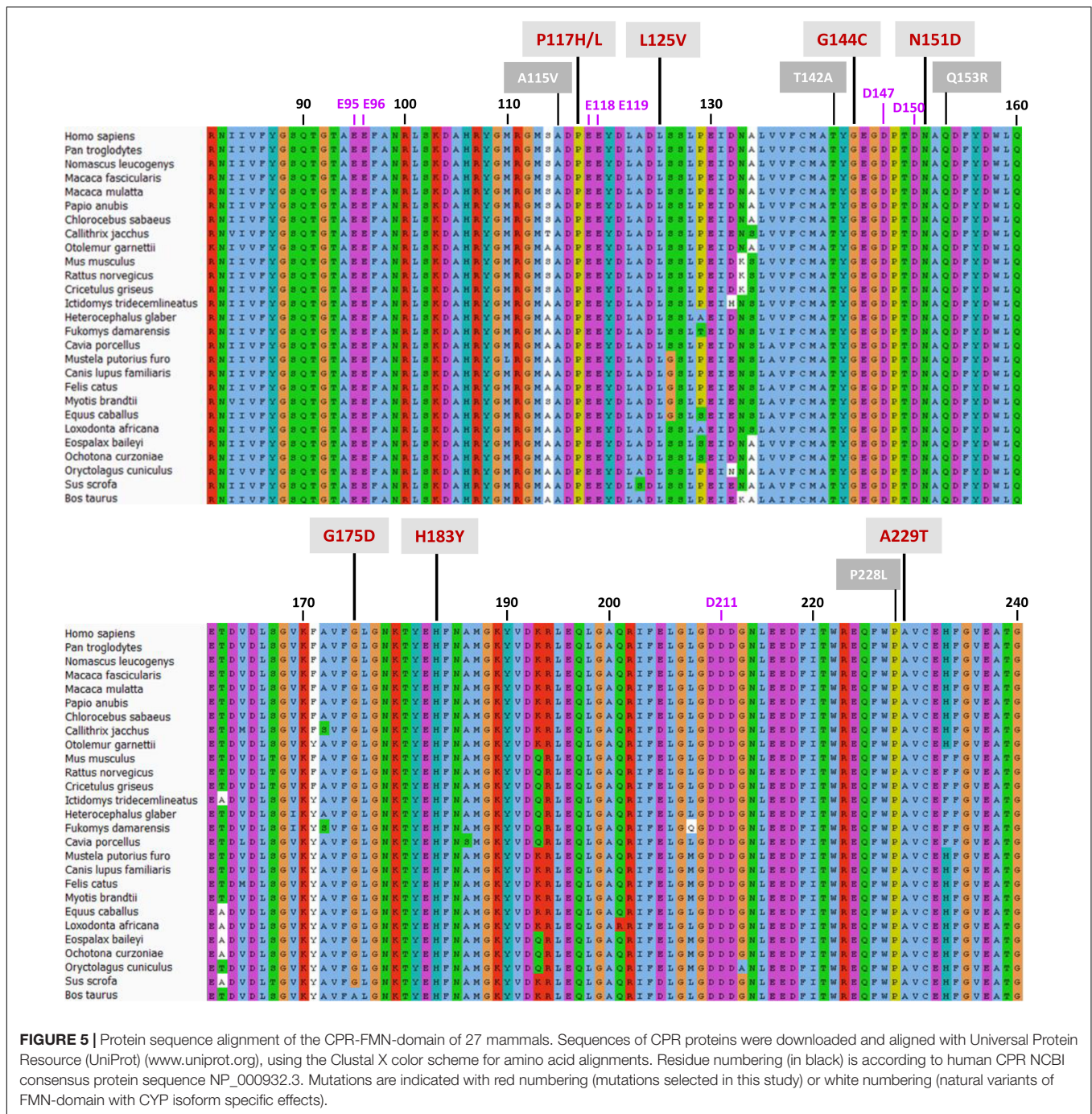
All selected FMN-domain mutations induced an increase in reaction velocity (Figure 1). The obtained CYB5 competition data seems to be indicative of an improved interaction of the FMN-domain mutants with their respective CYPs, in particular those for CYP2A6 and 3A4 and less clearly for CYP1A2, in particular for CPR mutant A229T. The CYB5 effect is rather small for CPR_{wt} and CPR_{mut} combined with CYP1A2, which may hinder the detection of possible binding differences between wild type and mutant CPRs. Indeed the ability of CYB5 to bind CYP and to compete with CPR has recently been demonstrated by NMR studies to be dependent on multiple factors including the effect of the substrate bound and membrane anchoring (Gentry et al., 2018, 2019). In this respect, our data regarding the use of two different CYP1A2 substrates seem to indicate that the substrate bound may have a modulating role in CPR_{mut} binding. This could be due to the fact that CYP's substrate binding site is considered to be rather malleable, and due to its close proximity may influence the architecture of the CPR binding site.

To assess if improved interactions of the FMN-domain mutants with their respective CYPs could be primarily caused by increased ionic interactions, changes in the salt profiles were also examined. Our data showed that this was mainly the case



for the CPR mutants selected with CYP2A6. CYB5's binding site on CYP is similar and overlaps with that of CPR. In addition, it is mainly guided by ionic interactions through CYB5 acidic surface residues (Waskell and Kim, 2015). Interestingly, CPR interactions with the most CYB5-sensitive of the three CYPs (CYP2A6, **Figure 3B**), demonstrated a strong difference in the ionic strength activity dependence, being poorly or very sensitive to increased NaCl concentrations with CPR_{wt} or CPR_{mut} , respectively (**Figure 4B**). Conversely, CYP1A2 and 3A4 demonstrated high and intermediate ionic strength sensitivities that are indistinguishable between CPR_{wt} and CPR_{mut} and these two CYPs are respectively poorly or intermediately stimulated by CYB5. Therefore, it seems that CYB5's capability to compete with CPR for CYP-binding (i.e., ability to stimulate) depends partly on the level of ionic interactions in the CPR:CYP complex, which our former (Campelo et al., 2018) and current data

demonstrated to be CYP-isoform dependent. Dependence of CPR activities on ionic strength is in part due to changes in the CPR conformational equilibrium. The superimposable salt profiles for the various CPR mutants specific for CYP1A2 and CYP3A4 might indicate that the effects of mutations: (i) do not have impact in the CPR conformational equilibrium and/or, (ii) might be attributed either to a change in salt interactions that could be obscured by the large ionic strength dependency of the CYPs activities or, alternatively, to improved binding through non-ionic interactions. Improved ionic strength interactions of FMN-domain mutants obtained with CYP2A6 (P117L/L125V, G175D, and H183Y) seem to be clear for the G175D mutant, creating an additional negative charge. However this is not directly obvious for the remaining mutations (P117L/L125V and H183Y). Still, subtle structural alterations induced by mutations may modulate charged residues in their vicinity to come into play.

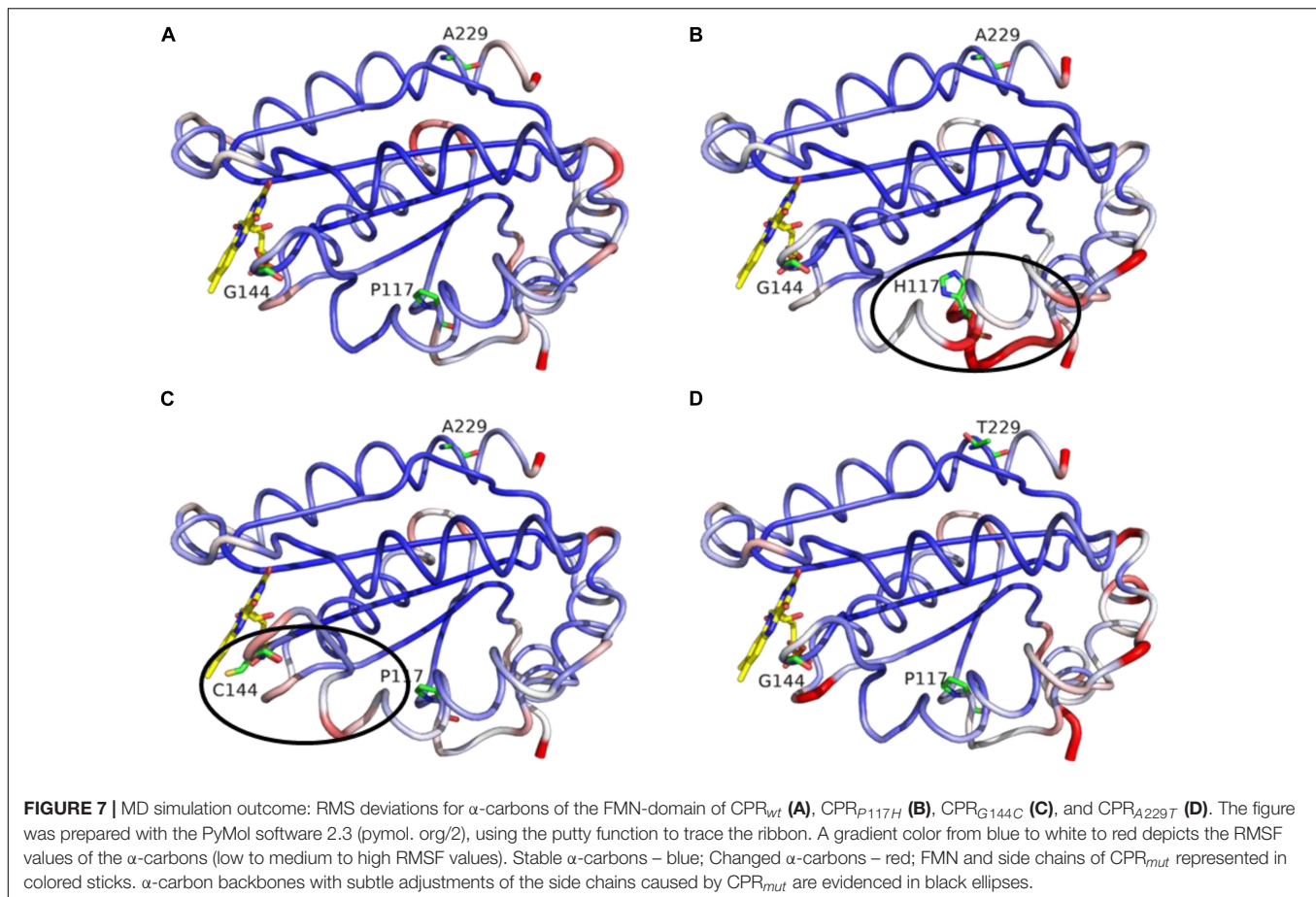


Small deviations might be translated in substantial structural effects (Waskell and Kim, 2015).

Mutations Co-localized With Structural Features Involved in CPR:CYP Interaction

Some of the identified mutations seem to cluster with patches of charged residues of the FMN-domain (Figure 5). For example, positions P117, N151, and G144 are in close vicinity to negatively

charged residues D116, E118, E119, E145, D147, and D150 (Figure 6) which have been formerly suggested to play a role in CPR:CYP interactions (Shen and Strobel, 1994; Wang et al., 1997; Zhao et al., 1999; Hamdane et al., 2009; Hong et al., 2010; Jang et al., 2010). Additionally, two mutated positions (G144 and H183) were found adjacent to the conserved tyrosine residues, Y143 and Y181, considered to be directly involved in FMN binding (Shen et al., 1989; Marohnic et al., 2010; Xia et al., 2011) (Figure 6). The G144C and H183Y substitutions may induce subtle alterations in the surface presentation of this cofactor,



Figures 6A and 6C) and the P117H substitution (compare Figures 6A and 6B). The relative rigidity of the Rossmann fold and involvement of multiple residues on several loops of the FMN domain upon interaction with CYP has recently been reported by elegant NMR studies by the group of Ayyalusamy Ramamoorthy (Prade et al., 2018; Gentry et al., 2019). Our data implies that the changes induced by the mutants probably propagate to the sidechains with minor changes on the backbone. Such effect is not unusual for the CYP enzyme complex, as recently described for the CYP1A1 enzyme, in which substrate binding was accommodated by minimal perturbation of the α -carbon backbone with subtle adjustments of the side chains (Bart and Scott, 2018). Additionally, a single amino acid change in a redox partner of CYP106A2 induced a considerable increase in substrate conversion by this bacterial CYP, with a minimal conformational perturbation (Sagadin et al., 2019).

CONCLUSION

Our results seem to suggest that every CYP is interacting with CPR in a specific manner, making use in an isoform specific mode, of docking elements, i.e., a composite of binding motifs of the FMN-domain. Therefore, the capacity of CPR to interact with so many CYPs can be attributed to the presence of different open

conformations which are affinity-sampled through the different binding motifs, by which each binding partner can be supplied with electrons. Altering or modifying the composition of open conformations (as we have shown recently in Campelo et al., 2018) and/or modifying these binding motifs, i.e., in the vicinity or within, will alter interaction with a particular redox partner. It is likely that some of these binding motifs are more common, i.e., shared among different CYPs, while others are more relevant for a specific CYP. Some of these FMN binding motifs might not yet been identified, and we hypothesize that one may be present around the P228-L229 positions.

Natural occurring variations of these CPR motifs may alter CYP-activity profiles, with the potential of causing specific genetic susceptibilities and pathologies. Drugs are metabolized for their excretion, frequently with involvement of multiple CYP isoforms. Natural occurring FMN-domain variants of these motifs may change the relative involvement of CYP isoforms, leading to altered metabolic profiles. In turn, this may potentially be related to lack of efficacy in drug treatment and/or adverse drug reactions. Likewise, genetic variations of residues forming the FMN-domain motifs may influence specific CYPs involved in steroidogenesis. Naturally occurring variants of the *POR* gene encoding CPR have been linked to a broad spectrum of human diseases, ranging from severe skeletal malformation and perturbed steroidogenesis (Antley-Bixler syndrome; OMIM

reference # 201750) to phenotypical normal individuals with, e.g., infertility (Tee et al., 2011). Former studies have made suggestions how mutations found in several natural occurring variants might interfere with the CPR:CYP interactions (reviewed in, Pandey and Flück, 2013; Burkhard et al., 2017). Our data seem to further underpin mechanistically these suggestions and the pathological consequences of these *POR* mutations.

AUTHOR'S NOTE

The authors dedicate this research to the memory of Dr. Henry W. Strobel.

DATA AVAILABILITY STATEMENT

All datasets generated for this study are included in the article/**Supplementary Material**.

AUTHOR CONTRIBUTIONS

FE, GT, and MK: planning experiments. FE, DC, BG, and SB: performed experiments. All authors: data analysis and interpretation, writing, reviewing, editing of the manuscript, and approval to the final version of the manuscript. GT and MK:

REFERENCES

- Aigrain, L., Pompon, D., Moréra, S., and Truan, G. (2009). Structure of the open conformation of a functional chimeric NADPH cytochrome P450 reductase. *EMBO Rep.* 10, 742–747. doi: 10.1038/embor.2009.82
- Barnaba, C., Gentry, K., Sumangala, N., and Ramamoorthy, A. (2017). The catalytic function of cytochrome P450 is entwined with its membrane-bound nature. *F1000Res.* 6:662. doi: 10.12688/f1000research.11015.1
- Barnaba, C., and Ramamoorthy, A. (2018). Picturing the membrane-assisted choreography of cytochrome P450 with lipid nanodiscs. *Chemphyschem* 19, 2603–2613. doi: 10.1002/cphc.201800444
- Bart, A. G., and Scott, E. E. (2017). Structural and functional effects of cytochrome *b5* interactions with human cytochrome P450 enzymes. *J. Biol. Chem.* 292, 20818–20833. doi: 10.1074/jbc.RA117.000220
- Bart, A. G., and Scott, E. E. (2018). Structures of human cytochrome P450 1A1 with bergamottin and erlotinib reveal active-site modifications for binding of diverse ligands. *J. Biol. Chem.* 293, 19201–19210. doi: 10.1074/jbc.RA118.005588
- Bernhardt, R., Ngoc Dao, N. T., Stiel, H., Schwarze, W., Friedrich, J., Jänig, G. R., et al. (1983). Modification of cytochrome P450 with fluorescein isothiocyanate. *Biochim. Biophys. Acta* 745, 140–148.
- Black, S. D., and Coon, M. J. (1982). Structural features of liver microsomal NADPH cytochrome P450 reductase. Hydrophobic domain, hydrophilic domain and connecting region. *J. Biol. Chem.* 257, 5929–5938.
- Black, S. D., French, J. S., Williams, C. H. Jr., and Coon, M. J. (1979). Role of a hydrophobic polypeptide in the N-terminal region of NADPH-cytochrome P450 reductase in complex formation with P450LM2. *Biochem. Biophys. Res. Commun.* 91, 1528–1535.
- Bridges, A., Gruenke, L., Chang, Y. T., Vakser, I. A., Loew, G., and Waskell, L. (1998). Identification of the binding site on cytochrome P450 2B4 for cytochrome *b5* and cytochrome P450 reductase. *J. Biol. Chem.* 273, 17036–17049.
- Burkhard, F. Z., Parween, S., Udhane, S. S., Flück, C. E., and Pandey, A. V. (2017). P450 Oxidoreductase deficiency: analysis of mutations and polymorphisms. *J. Steroid. Biochem. Mol. Biol.* 165, 38–50. doi: 10.1016/j.jsmb.2016.04.003

coordination and funding acquisition. All authors reviewed and gave approval to the final version of the manuscript.

FUNDING

This work was in part funded by a joint project, funded by the Portuguese *Fundação para a Ciência e a Tecnologia* [Grant FCT-ANR/BEXBCM/0002/2013 as well as Grant UID/BIM/0009/2016 of the Research Center for Toxicogenomics and Human Health (ToXomics)] and the *L'Agence Nationale de la Recherche* (Grant ANR-13-ISV5-0001). The high-throughput screening work was partly carried out with the equipment of PICT-ICEO facility (Toulouse, France), dedicated to the screening and the discovery of new and original enzymes. PICT-ICEO is supported by grants from the Région Midi-Pyrénées, the European Regional Development Fund and the Institut National de la Recherche Agronomique (INRA). FE was supported with a post-doctoral fellowship grant of the Portuguese *Fundação para a Ciência e a Tecnologia* (Grant SFRH/BPD/110633/2015).

SUPPLEMENTARY MATERIAL

The Supplementary Material for this article can be found online at: <https://www.frontiersin.org/articles/10.3389/fphar.2020.00299/full#supplementary-material>

- Campelo, D., Esteves, F., Brito Palma, B., Costa Gomes, B., Rueff, J., Lautier, T., et al. (2018). Probing the role of the hinge segment of cytochrome P450 oxidoreductase in the interaction with cytochrome P450. *Int. J. Mol. Sci.* 19:E3914. doi: 10.3390/ijms19123914
- Campelo, D., Lautier, T., Urban, P., Esteves, F., Bozonnet, S., Truan, G., et al. (2017). The hinge segment of human NADPH-cytochrome P450 reductase in conformational switching: the critical role of ionic strength. *Front. Pharmacol.* 8:755. doi: 10.3389/fphar.2017.00755
- Denisov, I. G., and Sligar, S. G. (2017). Nanodiscs in membrane biochemistry and biophysics. *Chem. Rev.* 117, 4669–4713.
- Duarte, M. P., Palma, B. B., Gilep, A. A., Laires, A., Oliveira, J. S., Usanov, S. A., et al. (2005). The stimulatory role of human cytochrome *b5* in the bioactivation activities of human CYP1A2, 2A6 and 2E1: a new cell expression system to study cytochrome P450 mediated biotransformation. *Mutagenesis* 20, 93–100.
- Duarte, M. P., Palma, B. B., Gilep, A. A., Laires, A., Oliveira, J. S., Usanov, S. A., et al. (2007). The stimulatory role of human cytochrome *b5* in the bioactivation activities of human CYP1A2, 2A6 and 2E1: a new cell expression system to study cytochrome P450-mediated biotransformation (a corrigendum report on Duarte et al. (2005) *Mutagenesis* 20, 93–100). *Mutagenesis* 22, 75–81.
- Ellis, J., Gutierrez, A., Barsukov, I. L., Huang, W. C., Grossmann, J. G., and Roberts, G. C. (2009). Domain motion in cytochrome P450 reductase: conformational equilibria revealed by NMR and small-angle x-ray scattering. *J. Biol. Chem.* 284, 36628–36637. doi: 10.1074/jbc.M109.054304
- Esteves, F., Campelo, D., Urban, P., Bozonnet, S., Lautier, T., Rueff, J., et al. (2018). Human cytochrome P450 expression in bacteria: Whole-cell high-throughput activity assay for CYP1A2, 2A6 and 3A4. *Biochem. Pharmacol.* 158, 134–140. doi: 10.1016/j.bcp.2018.10.006
- Fisher, C. W., Caudle, D. L., Martin-Wixtrom, C., Quattrocchi, L. C., Tukey, R. H., Waterman, M. R., et al. (1992). High-level expression of functional human cytochrome P450 1A2 in *Escherichia coli*. *FASEB J.* 6, 759–764.
- Frago, S., Lans, I., Navarro, J. A., Hervás, M., Edmondson, D. E., De la Rosa, M. A., et al. (2010). Dual role of FMN in flavodoxin function: electron transfer cofactor and modulation of the protein-protein interaction surface. *Biochim. Biophys. Acta* 1797, 262–271. doi: 10.1016/j.bbabi.2009.10.012

- Frances, O., Fatemi, F., Pompon, D., Guittet, E., Sizun, C., Pérez, J., et al. (2015). A well-balanced preexisting equilibrium governs electron flux efficiency of a multidomain diflavin reductase. *Biophys. J.* 108, 1527–1536. doi: 10.1016/j.bpj.2015.01.032
- Gentry, K. A., Anantharamaiah, G. M., and Ramamoorthy, A. (2019). Probing protein-protein and protein-substrate interactions in the dynamic membrane-associated ternary complex of cytochromes P450, b5, and reductase. *Chem. Commun.* 55, 13422–13425. doi: 10.1039/c9cc05904k
- Gentry, K. A., Zhang, M., Im, S. C., Waskell, L., and Ramamoorthy, A. (2018). Substrate mediated redox partner selectivity of cytochrome P450. *Chem. Commun.* 54, 5780–5783.
- Guengerich, F. P. (2015). “Human cytochrome P450 enzymes,” in *Cytochrome P450: Structure, Mechanism, and Biochemistry*, 4th Edn, ed. P. R. O. De Montellano (Basel: Springer), 523–785.
- Gum, J. R., and Strobel, H. W. (1981). Isolation of the membrane binding peptide of NADPH cytochrome P450 reductase. Characterization of the peptide and its role in the interaction of reductase with cytochrome P450. *J. Biol. Chem.* 256, 7478–7486.
- Gutierrez, A., Paine, M., Wolf, C. R., Scrutton, N. S., and Roberts, G. C. (2002). Relaxation kinetics of cytochrome P450 reductase: internal electron transfer is limited by conformational change and regulated by coenzyme binding. *Biochemistry* 41, 4626–4637.
- Hamdane, D., Xia, C., Im, S. C., Zhang, H., Kim, J., and Waskell, L. (2009). Structure and function of an NADPH cytochrome P450 oxidoreductase in an open conformation capable of reducing cytochrome P450. *J. Biol. Chem.* 284, 11374–11384. doi: 10.1074/jbc.M807868200
- Hlavica, P. (2015). Mechanistic basis of electron transfer to cytochromes p450 by natural redox partners and artificial donor constructs. *Adv. Exp. Med. Biol.* 851, 247–297. doi: 10.1007/978-3-319-16009-2_10
- Hlavica, P., and Lehnerer, M. (2010). Oxidative biotransformation of fatty acids by cytochromes P450: predicted key structural elements orchestrating substrate specificity, regioselectivity and catalytic efficiency. *Curr. Drug Metab.* 11, 85–104.
- Hlavica, P., Schulze, J., and Lewis, D. F. (2003). Functional interaction of cytochrome P450 with its redox partners: a critical assessment and update of the topology of predicted contact regions. *J. Inorg. Biochem.* 96, 279–297.
- Hong, Y., Li, H., Yuan, Y. C., and Chen, S. (2010). Sequence-function correlation of aromatase and its interaction with reductase. *J. Steroid. Biochem. Mol. Biol.* 118, 203–206. doi: 10.1016/j.jsbmb.2009.11.010
- Jang, H. H., Jamakhandi, A. P., Sullivan, S. Z., Yun, C. H., Hollenberg, P. F., and Miller, G. P. (2010). Beta sheet 2-alpha helix C loop of cytochrome P450 reductase serves as a docking site for redox partners. *Biochim. Biophys. Acta* 1804, 1285–1293. doi: 10.1016/j.bbapap.2010.02.003
- Johnston, W. A., Huang, W., De Voss, J. J., Hayes, M. A., and Gillam, E. M. (2008). Quantitative whole-cell cytochrome P450 measurement suitable for high-throughput application. *J. Biomol. Screen.* 13, 135–141. doi: 10.1177/1087057107312780
- Kandel, S. E., and Lampe, J. N. (2014). Role of protein-protein interactions in cytochrome P450-mediated drug metabolism and toxicity. *Chem. Res. Toxicol.* 27, 1474–1486. doi: 10.1021/tx500203s
- Kranendonk, M., Marohnic, C. C., Panda, S. P., Duarte, M. P., Oliveira, J. S., Masters, B. S., et al. (2008). Impairment of human CYP1A2-mediated xenobiotic metabolism by Antley-Bixler syndrome variants of cytochrome P450 oxidoreductase. *Arch. Biochem. Biophys.* 475, 93–99. doi: 10.1016/j.abb.2008.04.014
- Kranendonk, M., Mesquita, P., Laires, A., Vermeulen, N. P., and Rueff, J. (1998). Expression of human cytochrome P450 1A2 in *Escherichia coli*: a system for biotransformation and genotoxicity studies of chemical carcinogens. *Mutagenesis* 13, 263–269.
- Marohnic, C. C., Panda, S. P., McCammon, K., Rueff, J., Masters, B. S., and Kranendonk, M. (2010). Human cytochrome P450 oxidoreductase deficiency caused by the Y181D mutation: molecular consequences and rescue of defect. *Drug Metab. Dispos.* 38, 332–340. doi: 10.1124/dmd.109.030445
- McCammon, K. M., Panda, S. P., Xia, C., Kim, J. J., Moutinho, D., Kranendonk, M., et al. (2016). Instability of the human cytochrome P450 reductase A287P variant is the major contributor to its antley-bixler syndrome-like phenotype. *J. Biol. Chem.* 291, 20487–20502. doi: 10.1074/jbc.M116.716019
- McCullum, E. O., Williams, B. A., Zhang, J., and Chaput, J. C. (2010). Random mutagenesis by error-prone PCR. *Methods Mol. Biol.* 634, 103–109. doi: 10.1007/978-1-60761-652-8_7
- Miyamoto, M., Yamashita, T., Yasuhara, Y., Hayasaki, A., Hosokawa, Y., Tsujino, H., et al. (2015). Membrane anchor of cytochrome p450 reductase suppresses the uncoupling of cytochrome H.P450. *Chem. Pharm. Bull.* 63, 286–294. doi: 10.1248/cpb.c15-00034
- Miyazaki, K. (2011). MEGAWHOP cloning: a method of creating random mutagenesis libraries via megaprimer PCR of whole plasmids. *Methods Enzymol.* 498, 399–406. doi: 10.1016/B978-0-12-385120-8.00017-6
- Moutinho, D., Marohnic, C. C., Panda, S. P., Rueff, J., Masters, B. S., and Kranendonk, M. (2012). Altered human CYP3A4 activity caused by Antley-Bixler syndrome-related variants of NADPH-cytochrome P450 oxidoreductase measured in a robust in vitro system. *Drug Metab. Dispos.* 40, 754–760. doi: 10.1124/dmd.111.042820
- Nadler, S. G., and Strobel, H. W. (1991). Identification and characterization of an NADPH-cytochrome P450 reductase derived peptide involved in binding to cytochrome P450. *Arch. Biochem. Biophys.* 290, 277–284.
- Otey, C. R. (2003). “High-throughput carbon monoxide binding assay for cytochromes P450,” in *Methods in Molecular Biology*, Vol. vol. 230, eds F. H. Arnold, and G. Georgiou (Totowa, NJ: Humana Press), 137–139.
- Palma, B. B., Silva, E., Sousa, M., Urban, P., Rueff, J., and Kranendonk, M. (2013). Functional characterization of eight human CYP1A2 variants: the role of cytochrome b5. *Pharmacogenet. Genomics* 23, 41–52. doi: 10.1097/FPC.0b013e32835c2ddf
- Palma, B. B., Silva, E., Sousa, M., Vosmeer, C. R., Lastdrager, J., Rueff, J., et al. (2010). Functional characterization of eight human cytochrome P450 1A2 gene variants by recombinant protein expression. *Pharmacogenomics J.* 10, 478–488. doi: 10.1038/tpj.2010.2
- Pandey, A. V., and Flück, C. E. (2013). NADPH P450 oxidoreductase: structure, function, and pathology of diseases. *Pharmacol. Ther.* 138, 229–254. doi: 10.1016/j.pharmthera.2013.01.010
- Pikuleva, I. A., Cao, C., and Waterman, M. R. (1999). An additional electrostatic interaction between adrenodoxin and P450c27 (CYP27A1) results in tighter binding than between adrenodoxin and p450sc (CYP11A1). *J. Biol. Chem.* 274, 2045–2052.
- Prade, E., Mahajan, M., Im, S. C., Zhang, M., Gentry, K. A., Anantharamaiah, G. M., et al. (2018). A minimal functional complex of cytochrome P450 and FBD of cytochrome P450 reductase in nanodiscs. *Angew. Chem. Int. Ed. Engl.* 57, 8458–8462. doi: 10.1002/anie.201802210
- Rwera, F., Xia, C., Im, S., Haque, M. M., Stuehr, D. J., Waskell, L., et al. (2016). Mutants of cytochrome P450 reductase lacking either Gly-141 or Gly-143 destabilize its FMN semiquinone. *J. Biol. Chem.* 291, 14639–14661. doi: 10.1074/jbc.M116.724625
- Sagadin, T., Riehm, J., Putkaradze, N., Hutter, M. C., and Bernhardt, R. (2019). Novel approach to improve progesterone hydroxylation selectivity by CYP106A2 via rational design of adrenodoxin binding. *FEBS J.* 286, 1240–1249. doi: 10.1111/febs.14722
- Shen, A. L., and Kasper, C. B. (1995). Role of acidic residues in the interaction of NADPH-cytochrome P450 oxidoreductase with cytochrome P450 and cytochrome c. *J. Biol. Chem.* 270, 27475–27480.
- Shen, A. L., Porter, T. D., Wilson, T. E., and Kasper, C. B. (1989). Structural analysis of the FMN binding domain of NADPH-cytochrome P-450 oxidoreductase by site-directed mutagenesis. *J. Biol. Chem.* 264, 7584–7589.
- Shen, S., and Strobel, H. W. (1994). Probing the putative cytochrome P450- and cytochrome c-binding sites on NADPH-cytochrome P450 reductase by anti-peptide antibodies. *Biochemistry* 33, 8807–8812.
- Skandalis, A., Encell, L. P., and Loeb, L. A. (1997). Creating novel enzymes by applied molecular evolution. *Chem. Biol.* 4, 889–898.
- Strobel, H. W., Nadler, S. G., and Nelson, D. R. (1989). Cytochrome P-450: cytochrome P-450 reductase interactions. *Drug Metab. Rev.* 20, 519–533.
- Sündermann, A., and Oostenbrink, C. (2013). Molecular dynamics simulations give insight into the conformational change, complex formation, and electron transfer pathway for cytochrome p450 reductase. *Protein Sci.* 22, 1183–1195. doi: 10.1002/pro.2307

- Tee, M. K., Huang, N., Damm, I., and Miller, W. L. (2011). Transcriptional regulation of the human P450 oxidoreductase gene: hormonal regulation and influence of promoter polymorphisms. *Mol. Endocrinol.* 25, 715–731. doi: 10.1210/me.2010-0236
- Wang, M., Roberts, D. L., Paschke, R., Shea, T. M., Masters, B. S., and Kim, J. J. (1997). Three-dimensional structure of NADPH-cytochrome P450 reductase: prototype for FMN- and FAD-containing enzymes. *Proc. Natl. Acad. Sci. U.S.A.* 94, 8411–8416.
- Waskell, L., and Kim, J. J. (2015). “Electron transfer partners of cytochrome P450,” in *Cytochrome P450: Structure, Mechanism, and Biochemistry*, 4th Edn, ed. P. R. O. De Montellano (Basel: Springer), 33–68.
- Williams, P. A., Cosme, J., Sridhar, V., Johnson, E. F., and McRee, D. E. (2000). Mammalian microsomal cytochrome P450 monooxygenase: structural adaptations for membrane binding and functional diversity. *Mol. Cell* 5, 121–131.
- Xia, C., Panda, S. P., Marohnic, C. C., Martásek, P., Masters, B. S., and Kim, J. J. (2011). Structural basis for human NADPH-cytochrome P450 oxidoreductase deficiency. *Proc. Natl. Acad. Sci. U.S.A.* 108, 13486–13491. doi: 10.1073/pnas.1106632108
- Yun, C. H., Ahn, T., and Guengerich, F. P. (1998). Conformational change and activation of cytochrome P450 2B1 induced by salt and phospholipid. *Arch. Biochem. Biophys.* 356, 229–238.
- Yun, C. H., Song, M., Ahn, T., and Kim, H. (1996). Conformational change of cytochrome P450 1A2 induced by sodium chloride. *J. Biol. Chem.* 271, 31312–31316.
- Zhang, H., Im, S. C., and Waskell, L. (2007). Cytochrome *b5* increases the rate of product formation by cytochrome P450 2B4 and competes with cytochrome P450 reductase for a binding site on cytochrome P450 2B4. *J. Biol. Chem.* 282, 29766–29776.
- Zhao, Q., Modi, S., Smith, G., Paine, M., McDonagh, P. D., Wolf, C. R., et al. (1999). Crystal structure of the FMN-binding domain of human cytochrome P450 reductase at 1.93 Å resolution. *Protein Sci.* 8, 298–306.

Conflict of Interest: The authors declare that the research was conducted in the absence of any commercial or financial relationships that could be construed as a potential conflict of interest.

Copyright © 2020 Esteves, Campelo, Gomes, Urban, Bozonnet, Lautier, Rueff, Truan and Kranendonk. This is an open-access article distributed under the terms of the Creative Commons Attribution License (CC BY). The use, distribution or reproduction in other forums is permitted, provided the original author(s) and the copyright owner(s) are credited and that the original publication in this journal is cited, in accordance with accepted academic practice. No use, distribution or reproduction is permitted which does not comply with these terms.